Chemical Science & Engineering Research

Ariviyal Publishing

Research Article

DOI: 10.36686/Ariviyal.CSER.2021.03.07.034

Chem. Sci. Eng. Res., 2021, 3(7), 16-23.

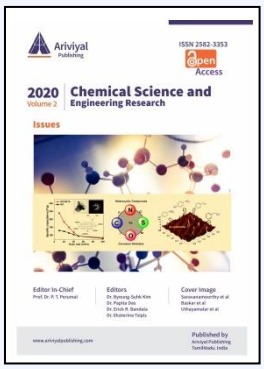

Adsorption of Phenol from Wastewater using Copper Oxide Supported on Activated Carbon Obtained from Coal: Thermodynamics and Kinetics Studies

Shehu Z.,[a] Danbature W. L.,*[a] Magaji B.,[a] Yakubu Y.S.[a] and Balarak D.[b]

[a]*Chemistry Department, Faculty of Science Gombe State University, Nigeria.*

[b]*Department of Environmental Health, Health Promotion Research Center, Zahedan University of Medical Sciences, Zahedan, Iran.*

***Corresponding author E-mail address**: wldanbature@mail.com (Danbature W. L.)

ISSN: 2582-3353

Crossref

Publication details
Received: 23th April 2021
Revised: 26th June 2021
Accepted: 26th June 2021
Published: 31st July 2021

Abstract: AC/CuO nanocomposite was synthesized using one pot procedure by using coal, Cupper (I) chloride as precursor for CuO and NaOH as precipitating and activating agents. The formation of AC/CuO nanocomposite was characterized and confirmed using UV -Visible spectroscopy, Scanning Electron Microscopy (SEM) and Fourier Transformed Infrared Spectroscopy (FTIR). The nanocomposite was used as an adsorbent for adsorption of phenol, and residual concentration was measured at a wavelength of 350 nm using UV -Visible spectrophotometer (model 6705). The effect of various parameters such as adsorbent dose, contact time, initial concentration, temperature and pH were investigated. AC-CuO nanocomposite adsorbent removed 99.995% of the phenol at optimum conditions of adsorbent dose: 0.1 g, contact time: 30 minutes, initial phenol concentration: 50 mg/L, temperature: 323K (50°C) and pH: 4. Gibbs free energy values for phenol adsorption were found to be 54.76, 56.57, 58.38, 60.19 and 62.00 kJ/mole at the temperature of 303, 313, 323, 333 and 343 K respectively. The positive values for Gibbs free energy indicate that the adsorption of Phenol on AC/CuO nanocomposite is non-spontaneous. The enthalpy and entropy change were found to be -0.0804 kJ/mole and -181.004 J/Kmole respectively. The negative value of enthalpy change indicates that the adsorption process is exothermic whereas the negative value for entropy change indicates decrease in randomness between Phenol- AC/CuO nanocomposite interfaces. Also, the adsorption process was found to follow pseudo-second order kinetic.

Keywords: Adsorption; Coal; Copper oxide Supported Activated Carbon; Kinetics; Phenol; Thermodynamics; Wastewater

1. Introduction

Incorporation of metals and metal oxides into carbonaceous materials greatly improve effectiveness and significance of the nanocomposite materials for wide applications. Thus, MnO_2/activated carbon (AC) composite[1] and bamboo-based activated carbon @ MnO_2 nanocomposites,[2] and activated carbon (AC)/metal oxides[3] were synthesized and found to have high electrochemical performance. Several studies reported impregnation of CuO on commercial activated carbon or prepared activated carbon from agricultural sources for adsorption of pollutants with improved adsorption efficiency than activated carbon alone. Hence, AC/CuO nanocomposite was used in removal of nitric oxide,[4] propanethiol,[5] gas desulphurization,[6] decolourization of reactive Orange 16[7] as well as adsorption of atrazine, caffeine and diclofenac.[8]

Modern industries such as textile, pharmaceutical, pesticide, dye manufacturing, paper making and petrochemical use phenol as raw material. Their industrial wastewater containing phenol is being discharged into aquatic environment with detriment to aquatic life. In human, phenol has been reported to cause nausea, erythema, deep necrosis.[9] Thus, attention of researchers has been drawn to control phenol in industrial wastewater before being discharged. Adsorption technique with the aid of activated carbon as adsorbent is the most common and effective method used in removal of phenol in wastewater.[9,10 -16] However, adsorption technique with the aid of adsorbents other than activated carbon such as vanillin,[17] magnetic mesoporous resorcinol–melamine–formaldehyde resin,[18] silica-based aerosols[19] as well as biodegradation by bacteria[20] has been used in removal of phenol in wastewater and were also found to be effective.

This study aimed to synthesize AC/CuO nanocomposite using one-pot procedure for removal of phenol. Coal was used as carbon source, Copper chloride as precursor for CuO and NaOH as precipitating and activating agents. The effect of various parameters such as adsorbent dose, contact time, initial concentration, temperature and pH were investigated using batch adsorption. Free energy, enthalpy change, entropy change, pseudo-first order and pseudo-second order kinetics for the adsorption of phenol were evaluated.

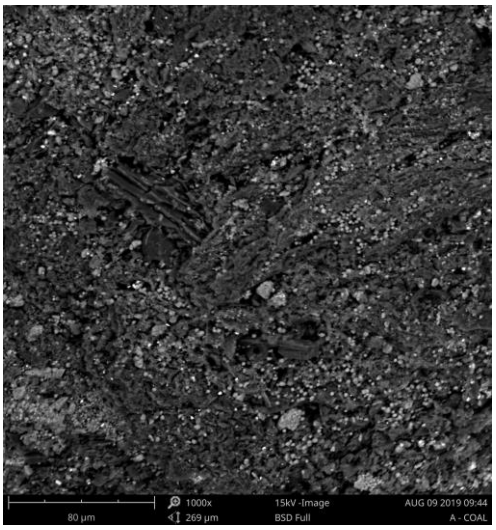

Fig. 1. SEM image of AC/CuO nanocomposite

2. MATERIALS AND METHODS

2.1. Materials

All reagents used were purchased from BDH and were of analytical grade. All glass wares were washed and dried overnight in an oven at 105°C. Total Ionic Strength Adjustment Buffer (TISAB) solution was used for pH adjustment. The un-absorbed adsorbate was determined with Ultraviolet–visible spectrophotometer (model 6705), and PerkinElmer Spectrum Version 10.0309 and SEM (Phenom World were used for characterization.

2.2. Collection and Preparation of Coal

The coal samples were collected from Maiganga area of Akko Local Government Area, Gombe State, Nigeria. The coal obtained was thoroughly washed with tap de-ionized water five times to remove dirts, and then dried in an oven at 105^{o}C for 1 hour. The coal was then crushed into smaller pieces with mortar and pestle.

2.3. One-pot Synthesis of AC/CuO Nanocomposite

The nanocomposite was synthesized according to the method used by some researchers[1-8] in which forty grams (40 g) of coal was weight and soaked in 160 ml of copper chloride (CuCl) and heated with constant stirring at 75^{o}C for 30 minutes. The color changed after 10 minutes of adding the coal from green to black color. After that, 80 ml of sodium hydroxide (NaOH) was added to activate the coal and to precipitate copper solution to CuO. The temperature was maintained at 75^{o}C for 30 minutes. The solution was allowed to settle down over night. The nanocomposite was simultaneously carbonized and calcinated in a muffle furnace wrapped with aluminium foil paper at 500^{o}C for 2 hours.

2.4. Adsorbents characterization

The adsorbent (AC/CuO nanocomposite) surface functional groups were obtained by the Fourier Transform Infrared Spectroscopy (FTIR, model Perkin Elmee Spectrum Version 10.0309) analysis over the range of 500–4000 cm^{-1}. The microstructure of the adsorbents was examined using a Scanning Electron Microscope (SEM, Phenom World). The maximum adsorption wavelength of the adsorbent was measured using UV-visible spectrophotometer (model 6705).

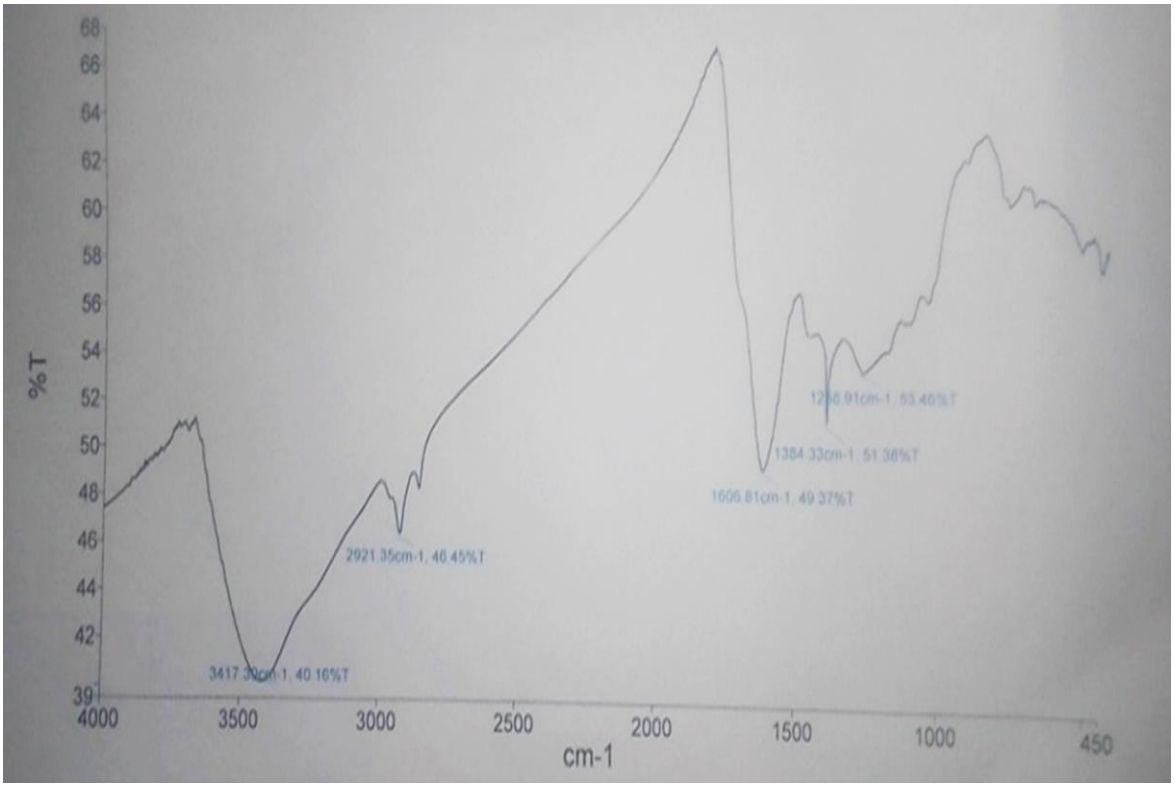

Fig. 2. FTIR spectrum for raw coal

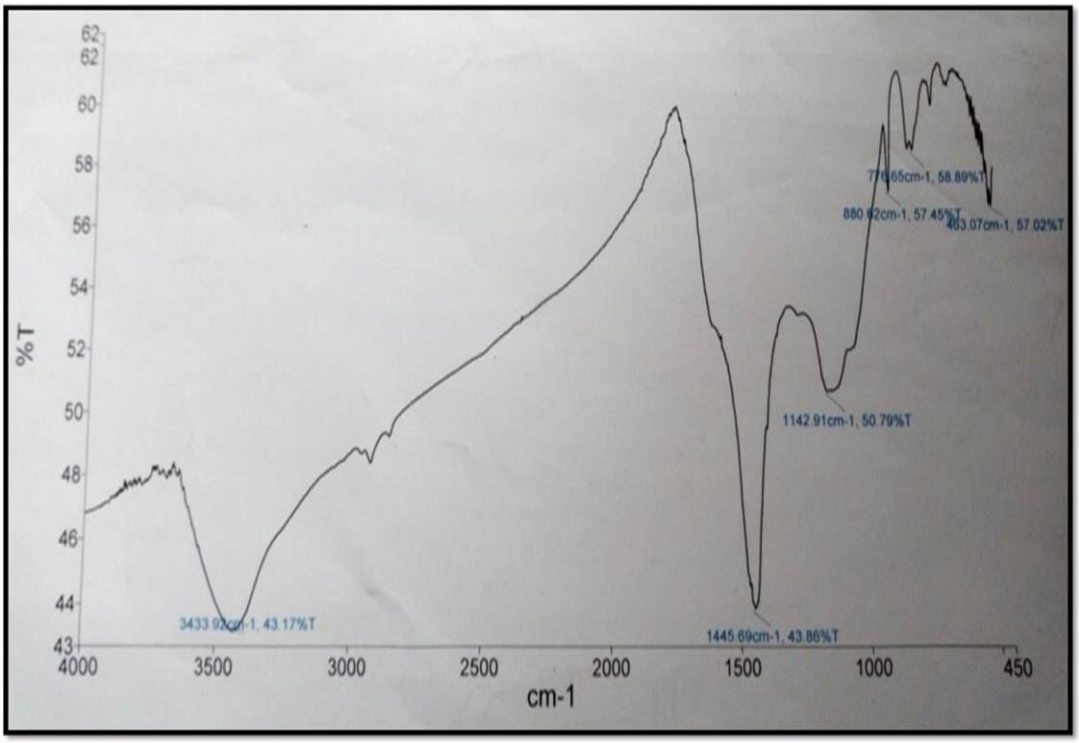

Fig. 3. FTIR spectrum for AC/CuO nanocomposite

2.5. Batch Adsorption of Phenol

Batch adsorption studies were carried out by investigating the effect of adsorbent dose, contact time, initial concentration, temperature and pH. For adsorbent dose, 0.1, 0.2, 0.3, 0.4, and 0.5 g of AC/CuO nanocomposite were each poured into five different beakers and 50 ml of phenol was added into each beaker. The contents were stirred for 30 minutes at room temperature and then filtered. The filtrate was then analyzed using UV-Spectrophotometer (model 6705) at the wavelength of 270 nm to determine the absorbance. The same procedures were followed for other effects by varying (10 to 60 minutes) for the contact time, (10 to 50mg/L) for the Initial concentration, (30^{o}C to 70^{o}C) for the temperature and (2 to 10) for the pH. 1M HCl and 1M NaOH were used for pH adjustment.

The amount of phenol adsorbed (q_e) on AC/CuO nanocomposite and the percentage removal of phenol red were calculated as:

$$q_e = (c_o - c_e)\frac{V}{W} \quad (1)$$

$$\% \text{ Removal} = (\frac{C_o - C_e}{C_o}) \times 100\% \quad (2)$$

Where C_o, C_e is the initial and equilibrium concentration (mg/L), respectively, V is the volume of the solution (L) and w is the amount of adsorbent (g).

3. Results and Discussions

3.1. SEM analysis

Fig. 1 showed SEM image of AC/CuO nanocomposite. The Scanning Electron Microscopy technique determines the size, shape and surface morphology with direct visualization of the nanoparticle. The surface morphology of the synthesized AC/CuO nanocomposites was investigated using SEM analysis. The SEM images of the AC/CuO nanocomposite showed porous structure consisting of coated structure. The coated dispersion on the surface of carbon showed the appearance of CuO nanoparticles. This description is in agreement with the work by some researchers.[1-8]

3.2. FTIR Result Analysis

Fig. 2 and Fig. 3 showed the FTIR spectra of the raw coal and AC/CuO nanocomposite respectively. For the raw coal, the absorption bands observed includes: 3417.92 cm^{-1}, 2921.35 cm^{-1}, 1258.91 cm^{-1}, 1384.33 cm^{-1} and 1606.81 cm^{-1}. In the FTIR analyses of raw coal, the band at 3417.30 cm^{-1} corresponds to the highly stretching symmetric of O-H stretching. Bands at 2921.35 cm^{-1} and 1606.81 cm^{-1} belongs to C-H and C=O bonds stretching respectively. Band at 1384.33 cm^{-1} belong to C-H bending mode of aliphatics while band at 1258.91 cm^{-1} belongs to C-O stretching. This is similar with FTIR spectra of coal reported by[21] FTIR analysis of AC/CuO nanocomposite showed peaks at 3417.92 cm^{-1}, 1445.69 cm^{-1}, 1142.91 cm^{-1}, 880.62 cm^{-1}, 776.65 cm^{-1} and 463.07 cm^{-1}. Peaks at 880.62 cm^{-1}, 776.65 cm^{-1} and 463.07 cm^{-1} can be assigned to the vibrations of the Cu-O stretching. This is also in agreement as reported by.[1] Whereas the bands at 3417.92 cm^{-1}, 1445.69 cm^{-1} and 1142.91 cm^{-1} belong to OH, C=O and C-O stretching vibrations.[22,23]

3.3. UV Visible Results

UV-Visible spectroscopy is a technique use for measuring the transmittance or absorbance of a sample as a purpose of the wavelength of electromagnetic radiation. The UV-Visible

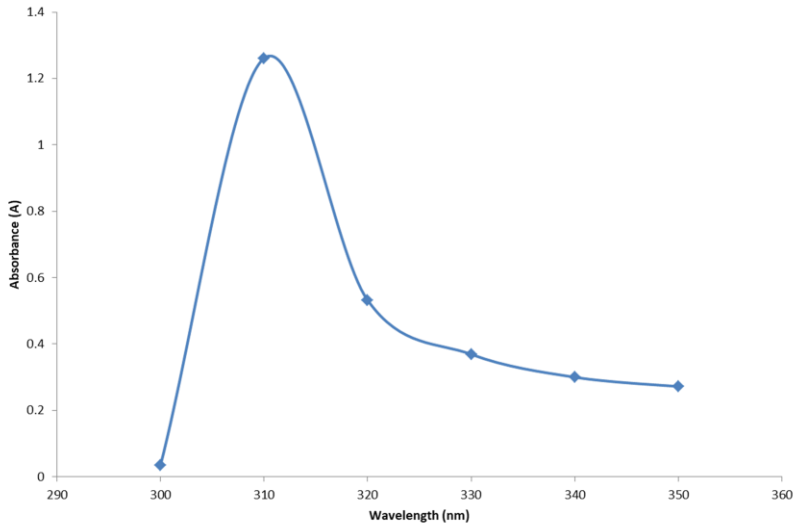

Fig. 4. Uv-visible spectrum of AC/CuO nanocomposite.

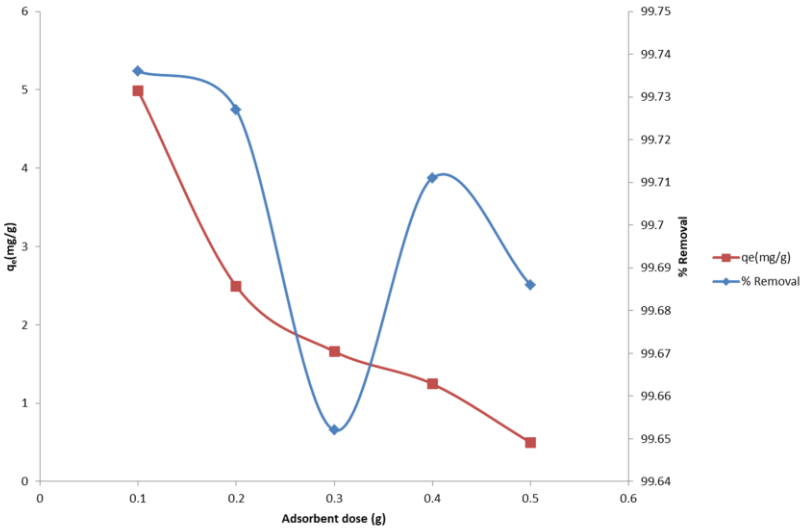

Fig. 5. Effects of adsorbent dose.

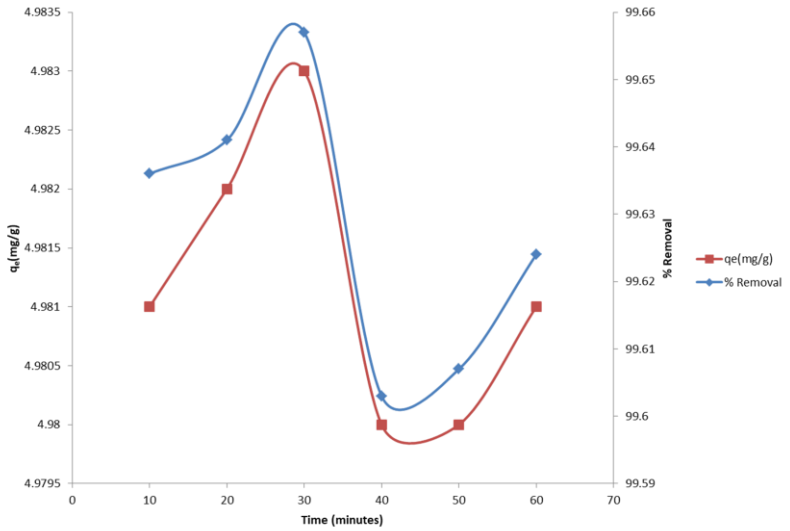

Fig. 6. Effect of contact time

spectrophotometer was used to measure the visual absorbances of the AC/CuO nanocomposite. This was carried out between 290 nm to 350 nm. The maximum absorption wavelength was found at 310 nm due to surface Plasmon resonance, Fig. 4. The maximum absorption wavelength has been reported to be 300 nm[23,24] for CuO nanoparticles and 310 nm for chitosan-CuO nanocomposite.[25] Hence, it could be concluded that the maximum absorption wavelength found at 310 nm for AC/CuO nanocomposite was due to CuO nanoparticles.

3.4. Effect of adsorbent dose on phenol

The percentage removal of the phenol by adsorption on to AC/CuO nanocomposite adsorbent was studied by varying the dosage of AC/CuO nanocomposite adsorbent in the range from 0.1 to 0.5 g, with a solution 10 mg/L of the phenol concentration, at shaking time of 60 minutes (1 hour), at a fixed pH of 7, room temperature of 30^{o}C. The result obtained was plotted as percentage removal and quantity absorbed of phenol against adsorbent dose respectively, Fig. 5. Generally, the removal percentage and adsorption capacity of phenol decreases with increase in AC/CuO nanocomposite dose. Thus, dose of the adsorbent having the optimum phenol red removal competence was found to be 0.1 g. Hence, 0.1 g of AC/CuO nanocomposite was taken as the dose of the material for the remaining experiment.

3.5. Effect of contact time on phenol

In adsorption method, contact time plays an important role than other adsorption effect. In order to study the effect of contact time on adsorption of phenol, the adsorption experiment were conducted by varying the time from 10 to 60 minutes, with a solution of 10 mg/L of phenol concentration, at a fixed pH of 7 and room temperature of 30^{o}C. The percent of removal of phenol increases with contact time until equilibrium at first 30 minutes and beyond this time the removal percentage decreases with increase in contact time, Fig. 6. Also, the adsorption capacity increases as the contact time increases until it reaches equilibrium from which the number of quantity absorbed start decreasing. The result corresponds to the work that was done by Madgda, et al.,(2014) which shows that the adsorption capacities of two adsorbents for phenol increases with increase in contact time at the beginning period.

3.6. Effect of initial concentration on phenol

Fig. 7 represents effect of initial phenol concentration. Both percentage removal and quantity adsorbed increases with increase in initial concentration of phenol. So the maximum efficiency was achieved at the initial concentration of 50 mg/L with the maximum percentage of (99.906%). At higher initial phenol concentration there was plateau formation and according to[10] the plateau indicates saturation of the available binding sites on the adsorbent.

3.7. Effect of temperature on phenol

Fig. 8 shows the relationship between temperature with percentage removal and adsorption capacity of phenol. At the temperature of 30^{o}C and 40^{o}C, the adsorption capacity and percentage removal of phenol on AC/CuO nanocomposite remains constant and slightly increases when the temperature increases to 50^{o}C. And beyond the temperature of 50^{o}C, the adsorption capacity and the percentage removal decreases with increase in temperature. Thus, optimum temperature was selected to be 50^{o}C.

3.8. Effect of pH on phenol

The effect of pH on phenol removal was studied by varying the pH from 2-10 under the optimum conditions (i.e dose of 0.1 g, time of 30 minutes, initial phenol concentration of 40 mg/L and at temperature of 50^{o}C). The results obtained were plotted as percentage removal and quantity absorbed against pH as shown in Fig. 9. At pH of 2, 4, 7, 8 and 10, the percentage removal was found to be 99.959, 99.995, 99.990, 99.986 and 99.938 % respectively. The removal of phenol is highly dependent on pH of the solution. In this result the pH was found to be at 4 with the maximum percentage of (99.995%) and thereafter start decreasing and the absorption capacity was found to be nearly equal. It was observed that in the acidic medium as the pH increased, the percentage removal increases. However, in the alkaline medium, percentage removal decreases with increase in pH. Interesting, at the pH of 7 (neutral), the percentage removal remains within the intermediary between acidic and alkaline medium.

3.9. Adsorption Kinetics

In this study, Pseudo-first order and Pseudo-second order kinetic models were studied as represented in equation 3 and 4 respectively.

$$Log(q_e - q_t) = Log\, q_e - \frac{K_1 t}{2.303} \quad (3)$$

$$\frac{t}{q_t} = \frac{1}{K_2 qe^2} - \frac{1}{q_e}\, t \quad (4)$$

Where K_1 (1/min) is the pseudo first order adsorption rate coefficient, q_e and q_t are the values of amount. Adsorbed per unit mass at equilibrium and at any time t, K_2 (g/mg min.) is the rate constant of second-order adsorption.

The pseudo first plot of Log (q_e - q_t) against time (t) should give a linear graph from which K_1 and q_e could be determined from the slope and intercept of the plot respectively. For pseudo second order, the plot of $\frac{t}{q_t}$ against time (t) should give a linear graph from which q_e and K_2 could be determined from the slope and intercept of the plot respectively.

From Table 1, the R^2 values of the two kinetic models are 0.0007 and 0.988 for pseudo-first-order and pseudo-second-order respectively. The R^2 values of the kinetic models suggest that the pseudo-second-order model mechanism fitted the experimental data. The closeness of q_e cal. and $q_{e\,exp}$. values for pseudo-second-order proved that the adsorption of phenol followed pseudo-second-order. Report by Mohammad et al.,(2015),[12] Magda et al., (2014), and Polat et al., (2006)[11] showed that adsorption of phenol on different adsorbent followed pseudo-second order.

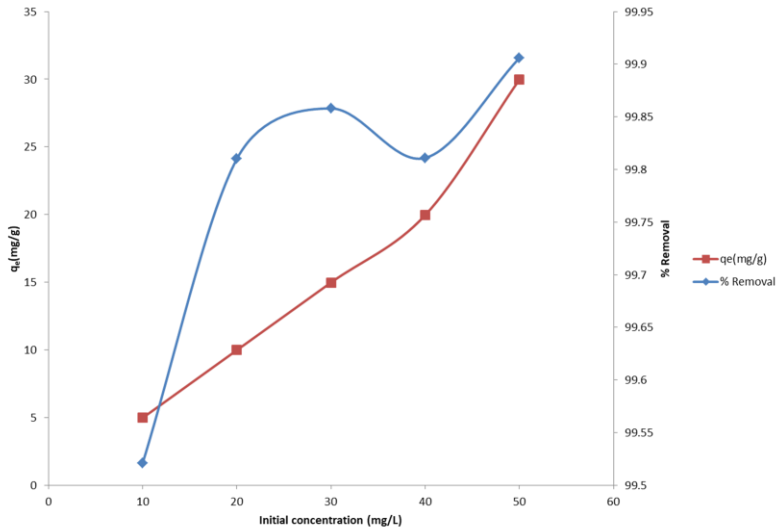

Fig. 7. Effect of initial phenol concentration

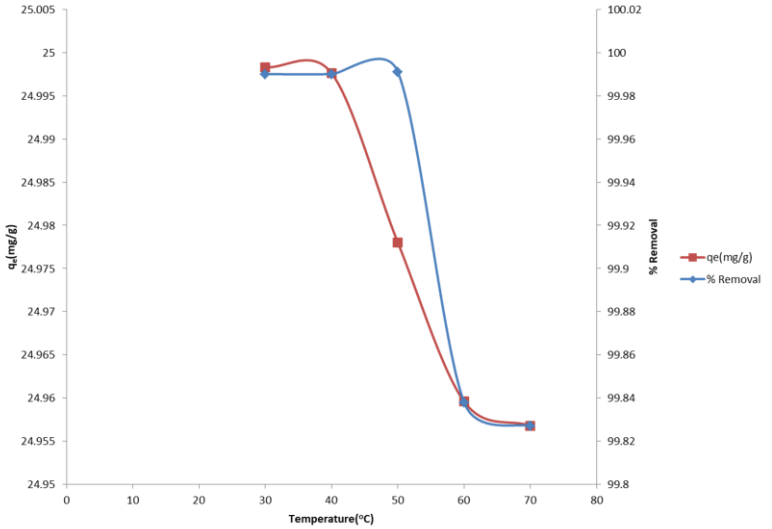

Fig. 8. Effect of temperature

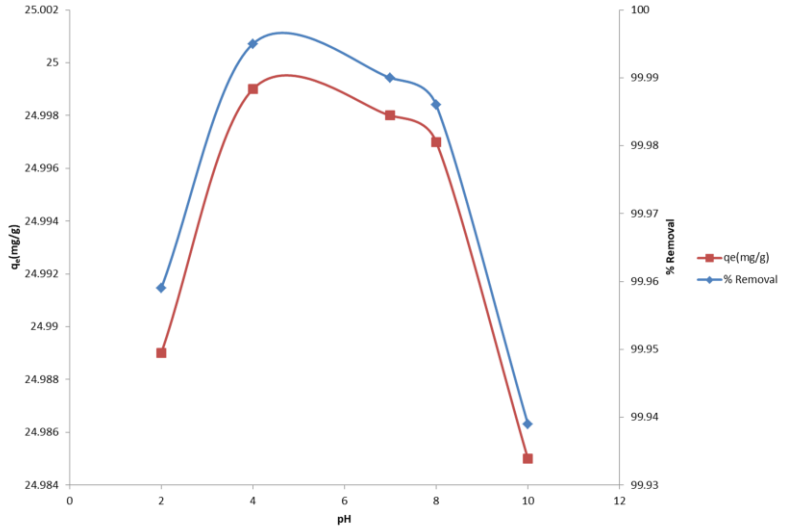

Fig. 9. Effect of pH

Table 1. Kinetic parameters results

Pseudo-second order		Pseudo-first order	
R^2	0.988	R^2	0.0007
K_2(g/mgmin)	0.2625	K_1(1/min.)	0.0039
$q_{e\ cal.(mg/g)}$	5.216	$q_{e\ cal.\ (mg/g)}$	0.0066
$q_{e\ exp.\ (mg/g)}$	4.983	$q_{e\ exp.\ (mg/g)}$	4.983

Table 2. Thermodynamic parameters of adsorption of phenol

T (K)	ΔG^0(kJ/mole)	ΔH^0(kJ/mole)	ΔS^0(J/mole/K)
303	54.76	-0.0804	-181.004
313	56.57		
323	58.38		
333	60.19		
343	62.00		

3.10. Thermodynamic Studies

Thermodynamic parameters such as standard free energy change (ΔG^o), standard enthalpy change (ΔH^o) and standard entropy change (ΔS^o) can be calculated using the following equation:.

$$\Delta G^o = -RTlnK_c \quad (5)$$

$$\Delta G^o = \Delta H - T\Delta S \quad (6)$$

$$lnK_c = \frac{\Delta S^o}{R} - \frac{\Delta H^o}{RT} \quad (7)$$

$$K_c = \frac{q_e}{c_e} \quad (8)$$

Where, K_c is equilibrium constant resulting from the ratio of the equilibrium concentrations of the phenol red on an adsorbent and in solution.

From equation 7, ΔH^o and ΔS^ocan be calculated from the slope and intercept of a plot of $\ln K_c$ versus 1/T and ΔG^o can be calculated from equation 6. The thermodynamic parameters of the phenol adsorption onto AC/CuO Nanocomposite are given in Table 2. The standard Gibbs free energies (ΔG^o) of adsorption were positive at all investigated temperatures. The positive values of ΔG^o of the adsorption confirmed that the adsorption of phenol onto AC/CuO nanocomposite was not spontaneous. However,[12] stated that the weak positive values of free energy change indicate that the process is feasible and the weaker values at lower temperatures imply that adsorption is favored at lower temperatures. The negative values of ΔH^o and ΔS^o indicates that the adsorption process is exothermic and there is decrease in randomness between phenol- AC/CuO Nanocomposite interfaces respectively. Similarly, adsorption of phenol on rice husk activated carbon gives negative values for both $\Delta \boldsymbol{H^o}$ and $\Delta \boldsymbol{S^o}$.[12]

4. Conclusions

In this work, the AC/CuO nanocomposites was synthesized successfully using mixing of solution method and characterized using various analytical apparatus like UV-Visible adsorption spectroscopy, SEM and FTIR. The UV-Visible analysis showed that the nanocomposite has its highest wavelength (λmax) at 310 nm. The structure and morphology of the nanocomposite were characterized using the scanning electron microscopy (SEM). The SEM images above proved rough structures and agglomeration nanocomposite, it also proved that the nanocomposites are matrix consisting of micro-sized AC/CuO nanocomposite having layered structure with irregular shape. Different functional groups in the AC/CuO nanocomposite were detected by the FTIR analysis and it shows the functional groups like; O-H, C-H, C-C, C-O-C and C-CuO. The removal of phenol using AC/CuO nanocomposite adsorbent has been carried out. From the investigation, it was observed that the experimental parameters such as adsorbent dose, contact time, initial concentration, temperature and pH were investigated for their prospective effect on the competence of phenol red and phenol removal. Based on the comprehensive experimental investigation, AC/CuO nanocomposite adsorbent also removed 99.995% of the phenol at optimum process conditions (adsorbent dose of 0.1 g, contact time of 30 minutes, initial phenol concentration of 50 mg/L, temperature of 323K (50°C) and pH of 4). These proposed that the adsorbent could be used for the phenol removal in wastewater.

Acknowledgements

The authors wish to thank Gombe State University for the provision of work space in the laboratory.

Conflicts of Interest

The authors declare no conflict of interest.

References

1 Wang J.W.; Chen Y.; Chen B.Z. A Synthesis Method of MnO_2/activated Carbon Composite for Electrochemical Supercapacitors. *J. Electrochem. Soc*., 2015, **162**, A1654. [CrossRef]
2 Huang T.; Qiu Z.; Wu D.; Hu, Z. Bamboo-based Activated Carbon@ MnO_2 Nanocomposites for Flexible High-performance Supercapacitor Electrode Materials. *Int. J. Electrochem. Sci.*, 2015, **10**, 6312-6323. [CrossRef]
3 Barroso-Bogeat A.; Alexandre-Franco M.; Fernandez-Gonzalez C.; Macías-García A; Gomez-Serrano V. Electrical Conductivity of Activated carbon–metal oxide Nanocomposites under Compression: A Comparison Study. *Phys. Chem. Chem. Phys*., 2014, **16**, 25161-25175. [CrossRef]
4 Ahmad N.; Yong S.H.; Ibrahim N.; Ali U.F.M.; Ridwan F.M.; Ahmad R. Optimisation of Copper Oxide Impregnation on Carbonised Oil Palm Empty Fruit Bunch for Nitric Oxide Removal using Response Surface Methodology. In E3S Web *Conf.*, 2018, **34**, 02029. EDP Sciences. [CrossRef]
5 Moreno-Pirajan J.C.; Tirano J.; Salamanca B.; Giraldo L. Activated Carbon Modified with Copper for Adsorption of Propanethiol. *Int. J. Mol. Sci*., 2010, **11**, 927-942. [CrossRef]
6 Yang Y.; Qian Y.H.; Xu C.H.; Jiang J.L.; Chen X.F. Characterization and Performance Test of Copper Oxide Supported on Activated Carbon and Attapulgite for Flue Gas Desulfurization. *Appl. Mech. Mater*., 2012, **184**, 1466-1470. [CrossRef]
7 Abdullah A.H.; Yuan W.W.; Yaziz M.I. Decolourisation of Reactive Orange 16 by Activated Carbon and Copper Oxide Catalysts Supported by Activated Carbon. *J. Phys. Sci.,* 2010, **21**, 29-40. [CrossRef]
8 Peternela J.; Silva M.F.; Vieira M.F.; Bergamasco R.; Vieira A.M.S. Synthesis and Impregnation of Copper Oxide Nanoparticles on Activated Carbon through Green Synthesis for Water Pollutant Removal. *Mater. Res*., 2017, **21**, e20160460. [CrossRef]

9 Feng J.; Shi S.; Pei L.; Lv J.; Liu Q.; Xie S. Preparation of Activated Carbon from Polygonum Orientale Linn. to Remove the Phenol in Aqueous Solutions. *Plos one*, 2016, **11**, e0164744. [CrossRef]
10 Akl M.A.; Dawy M.B.; Serage A.A. Efficient Removal of Phenol from Water Samples using Sugarcane Bagasse Based Activated Carbon. *J. Anal. Bioanal. Tech*., 2014, **5**, 1-12. [CrossRef]
11 Polat H.; Molva M.; Polat M. Capacity and Mechanism of Phenol Adsorption on Lignite. *Int. J. Miner. Process*., 2006, **79**, 264-273. [CrossRef]
12 Mohammad Y.S.; Egbenya M.; Sunday B.I.; Abdul-Raheem G.I.W.A.; Charles A.O. Isotherm, Kinetics and Thermodynamics of Phenol Adsorption onto Rice Husk Activated Carbon. *Leonardo El. J.*, 2015, 115-128. [CrossRef]
13 Kumar D.; Patidar R.; Girish C.R. Phenol Adsorption from Wastewater using Betel Nut Shell as Adsorbent. *Int. J. Civ. Eng. Technol.*, 2018, **9**, 467-474. [CrossRef]
14 Mubarak N.M.; Sazila N.; Nizamuddin S.; Abdullah E.C.; Sahu J.N. Adsorptive Removal of Phenol from Aqueous Solution by using Carbon Nanotubes and Magnetic Biochar. *NanoWorld J.*, 2017, **1**, 32-37. [CrossRef]
15 Abdel G.N.; EL Chaghaby G.A.; Helal F.S. Preparation, Characterization and Phenol Adsorption Capacity of Activated Carbons from African Beech Wood Sawdust. Global *J. Environ. Sci. Manage*., 2016, **2**, 209-222. [CrossRef]
16 Gupta V.K.; Tyagi I.; Agarwal S.; Singh R.; Chaudhary M.; Harit A.; Kushwaha S. Column Operation Studies for the Removal of Dyes and Phenols using a Low Cost Adsorbent. *Glob. J. Environ. Sci. Manage*., 2016, **2**, 1-10. [CrossRef]
17 Djunaidi M.C.; Dwi S.J. Selective Adsorption of Phenol and Vanillin using Eugenol based molecularly imprinted polymer, Proceedings of the 9th Joint Conference on Chemistry; Green Chemistry Section 3: Analytical Chemistry, Diponegoro University, 2015, 251-257. [Link]
18 Heydaripour J.; Gazi M.; Oladipo A.A.; Gulcan H.O. A Novel Magnetic Mesoporous Resorcinol–melamine–formaldehyde Resin for Removal of Phenols from Aqueous Solution. *J. Porous Mater*., 2019, **26**, 1249-1258. [CrossRef]
19 Matias T.; Marques J.; Quina M.J.; Gando-Ferreira L.; Valente A.J.; Portugal A.; Duraes L. Silica-based Aerogels as Adsorbents for Phenol-derivative Compounds. *Colloids Surf. A: Physicochem. Eng. Asp*, 2015, **480**, 260-269. [CrossRef]
20 Shahriari, M.M.; Safaei N.; Ebrahimipour G.H. Optimization of Phenol Biodegradation by Efficient Bacteria Isolated from Petrochemical Effluents. *Glob. J. Environ. Sci. Manage*., 2016, **2**, 249-256. [CrossRef]
21 Cuhadaroglu D.; Uygun O.A. Production and Characterization of Activated Carbon from a Bituminous Coal by Chemical Activation. *Afr. J. Biotechnol*., 2008, **7**, 3703-3710 [CrossRef]
22 Mopoung S.; Moonsri P.; Palas W.; Khumpai S. Characterization and Properties of Activated Carbon Prepared from Tamarind Seeds by KOH Activation for Fe (III) Adsorption from Aqueous Solution. *Sci. World J*., 2015, 1-9. [CrossRef]
23 Al-Qodah Z.; Shawabkah R. Production and Characterization of Granular Activated Carbon from Activated Sludge. *Braz. J. Chem. Eng*., 2009, **26**, 127-136. [CrossRef]
24 Logpriya S.; Bhuvaneshwari V.; Vaidehi D.; SenthilKumar R.P.; Malar R.N.; Sheetal B.P.; Amsaveni R.; Kalaiselvi M. Preparation and Characterization of Ascorbic Acid-mediated Chitosan–copper Oxide Nanocomposite for Anti-microbial, Sporicidal and Biofilm-inhibitory Activity. *J. Nanostruct. Chem*., 2018, **8**, 301-309. [CrossRef]
25 Rahman A.; Ismail A.; Jumbianti D.; Magdalena S.; Sudrajat H. Synthesis of Copper Oxide Nano Particles by using Phormidium Cyanobacterium. *Indones. J. Chem*., 2009, **9**, 355-360. [CrossRef]